Comparison of five soil organic matter decomposition models using data from a ^{14}C and ^{15}N labeling field experiment

Marc Pansu,[1] Pierre Bottner,[2] Lina Sarmiento,[3] and Klaas Metselaar[4]

Received 30 January 2004; revised 15 July 2004; accepted 12 August 2004; published 24 November 2004.

[1] Five alternatives of the previously published MOMOS model (MOMOS-2 to -6) are tested to predict the dynamics of carbon (C) and nitrogen (N) in soil during the decomposition of plant necromass. ^{14}C and ^{15}N labeled wheat straw was incubated over 2 years in fallow soils of the high Andean Paramo of Venezuela. The following data were collected: soil moisture, total ^{14}C and ^{15}N and microbial biomass (MB)-^{14}C and -^{15}N, daily rainfall, air temperature and total radiation. Daily soil moisture was predicted using the SAHEL model. MOMOS-2 to -4 (type 1 models) use kinetic constants and flow partitioning parameters. MOMOS-2 can be simplified to MOMOS-3 and further to MOMOS-4, with no significant changes in the prediction accuracy and robustness for total-^{14}C and -^{15}N as well as for MB-^{14}C and -^{15}N. MOMOS-5 (type 2 models) uses only kinetic constants: three MB-inputs (from labile and stable plant material and from humified compounds) and two MB-outputs (mortality and respiration constants). MOMOS-5 did not significantly change the total-^{14}C and -^{15}N predictions but markedly improved the predictive quality and robustness of MB-^{14}C and -^{15}N predictions (with a dynamic different from the predictions by other models). Thus MOMOS-5 is proposed as an accurate and ecologically consistent description of decomposition processes. MOMOS-6 extends MOMOS-5 by including a stable humus compartment for long-term simulations of soil native C and N. The improvement of the predictions is not significant for this 2-year experiment, but MOMOS-6 enables prediction of a sequestration in the stable humus compartment of 2% of the initially added ^{14}C and 5.4% of the added ^{15}N. *INDEX TERMS:* 1045 Geochemistry: Low-temperature geochemistry; 1055 Geochemistry: Organic geochemistry; 1615 Global Change: Biogeochemical processes (4805); 3210 Mathematical Geophysics: Modeling; *KEYWORDS:* decomposition, modeling, tracer experiment, soil organic matter, carbon, nitrogen, ^{14}C, ^{15}N, microbial biomass

Citation: Pansu, M., P. Bottner, L. Sarmiento, and K. Metselaar (2004), Comparison of five soil organic matter decomposition models using data from a ^{14}C and ^{15}N labeling field experiment, *Global Biogeochem. Cycles*, *18*, GB4022, doi:10.1029/2004GB002230.

1. Introduction

[2] Extending the knowledge of soil carbon and nitrogen cycles and improving its modeling remain a major challenge for land use management and prediction of the global C and N flows. The kinetics are generally described by assigning fractions of the soil organic matter (SOM) into compartments that are supposed to be qualitatively homogeneous and by quantifying C and N flows between these compartments. Natural or artificial isotopic tracer techniques are an essential tool to understand and model SOM systems. The tracer is generally introduced in a particular compartment, and is followed through the other compartments, assumed to behave as ideally mixed reservoirs. Then the pathways of the tracer reflect the functioning of the system. Sensitivity analysis (SA) is a complementary tool that was more recently used to analyze complex SOM systems [e.g., *Knorr and Heimann*, 2001; *Chimner et al.*, 2002; *Paul et al.*, 2003].

[3] A pioneer SOM decomposition model (a simple two compartment model) was proposed by *Hénin et al.* [1959]. Among the further published models, many were too complex to be easily validated, because theoretical compartments were often not measurable. The numerous physical, chemical and biological SOM fractionation procedures seldom allowed identification of theoretically defined compartments. A major step was achieved when *Jenkinson and Powlson* [1976] and *Anderson and Domsch* [1978] proposed new procedures to measure the microbial biomass pool (MB), a keystone to describe the SOM system. However, the structural identifiability analysis [*Cobelli et al.*, 1979] of the complex theoretical schemes remains a

[1]Institut de Recherche pour le Développement, Montpellier, France.
[2]Centre d'Ecologie Fonctionnelle et Evolutive, Centre National de la Recherche Scientifique, Montpellier, France.
[3]Instituto de Ciencias Ambientales y Ecológicas, Facultad de Ciencias, Universidad de los Andes, Mérida, Venezuela.
[4]Crop and Weed Ecology, Wageningen University and Research Centre, Wageningen, Netherlands.

0886-6236/04/2004GB002230$12.00

difficult task. The models are often tested by estimating their predictive quality using long-term experiments. This approach is explored by, for example, *Moorhead et al.* [1999], who compared four models, or by *Smith et al.* [1997], who compared the following 10 models: Roth-C [*Jenkinson*, 1990; *Jenkinson and Rayner*, 1977], Ncsoil [*Molina et al.*, 1983], Century [*Parton et al.*, 1987], Hurley pasture [*Thornley and Verberne*, 1989], Verberne/MOTOR [*Verberne et al.*, 1990], ITE forest [*Thornley*, 1991], Daisy [*Hansen et al.*, 1991], DNDC [*Li et al.*, 1994], Candy [*Franko et al.*, 1995], and SOMM [*Chertov and Komarov*, 1997]. The authors identified two groups, but for most of the compared models the prediction errors did not differ significantly. Thus, the model performance seems to be independent of their conceptual content, suggesting that some of them may be overparameterized.

[4] Data from a former ^{14}C and ^{15}N labeling experiment performed under controlled laboratory conditions enabled construction of an initial MOMOS-C [*Sallih and Pansu*, 1993] and MOMOS-N [*Pansu et al.*, 1998] models. The aim of the present work was to validate and improve the initial MOMOS model with data from a new ^{14}C and ^{15}N experiment performed under natural field conditions. This paper compares the predictive quality and analyzes the sensitivity of five new versions (Momos-2 to -6) derived from the initial proposal (1) through successive simplifications of the model structure (the models more complex or more parameterized than MOMOS-2 are not taken into account in this study) by suppressing some compartments or some decomposition pathways and (2) by highlighting the key functional role of the microbial biomass compartment.

2. Materials and Methods

2.1. Site of the Experiment

[5] The experiment was conducted at the paramo site of Gavidia (8°35′N–8°45′N, 70°52′W–70°57′W) in the Andes of Mérida (Mérida State, Venezuela) at an altitude of 3400 m. The mean annual precipitation is 1329 mm, with a dry season between November and March and a rainy season between April and October. The mean annual temperature is 8.5°C differing only by 1.5°C between the coldest and the warmest months but with a mean daily thermal amplitude of 10.5°C. The experiment was set up in (1) a 2-year-old fallow plot (F2y data series) with an estimated soil cover = 0.85 of mainly perennial herbs and (2) in a 7-year-old fallow plot (F7y data series) covered by the characteristic paramo giant rosettes and by shrubs (height = 1 to 1.5 m, estimated soil cover = 0.9, differing markedly from grassland). The soil (*humitropepts*, USA Soil Taxonomy) is loamy and well drained. In the 0- to 10-cm layer, sand = 54%, silt = 31%, clay = 15%, pH(H_2O) = 4.5, water-holding capacity (v/v) = 0.52 (mean values of the two experimental plots), C = 9.4% (plot F2y) and 8.8% (plot F7y), and N = 0.55% (F2y) and 0.56% (F7y). The high organic matter content explains the high water-holding capacity. The cultivation system is based on a long fallow period used for extensive grazing (generally lasting from 5 to 10 years) alternating with a short (1 to 3 years) potato and cereal cropping period.

2.2. ^{14}C and ^{15}N Labeled Plant Material

[6] A low N-requiring old cultivar of spring wheat (Florence Aurore) was grown from seed to maturity in a labeling chamber with controlled $^{14}CO_2$ atmosphere (0.03% v/v, 0.86 kBq mg^{-1} C), temperature, radiation, and alternate lighting conditions. The plants, which were cultivated in pure sand, were periodically flooded with a complete nutrient solution containing $Ca(^{15}NO_3)_2$ (10% atomic ratio) as the sole N source. At ear emergence the wheat was dried at 40°C. Only the stems and leaves were used in the experiment. They were ground into particles between 2 and 7 mm long and mixed to obtain a homogeneous material. The C content of the material was 43.0 ± 0.39% (0.821 ± 0.022 kBq mg^{-1} C), the N content was 1.60 ± 0.05% (^{15}N isotopic ratio = 9.250 ± 0.451%), and the C/N ratio was 26.9 ± 0.9. The biochemical fractions of the straw [*van Soest et al.*, 1991] were as follows: neutral detergent soluble = 0.36, hemicelluloses = 0.25, cellulose = 0.26, lignin = 0.03, and ashes = 0.10. The N content of the straw used in the present part of the experiment was relatively high, but the behavior of the model from a litter with low N content will be discussed elsewhere (work in preparation).

2.3. Field Incubation

[7] For each plot (F2y and F7y series), homogenized air-dried soil, sampled from the 5- to 10-cm layer, was divided into 40 samples of 150.0 g soil each. Then 3.260 g of labeled straw were homogeneously added to each sample, corresponding to 9.0% (F2y) and 9.6% (F7y) of total C (soil native C + plant material C) and 5.9% (F2y) and 5.8% (F7y) of total N (soil native N + plant N). The mixture was placed in 10 × 8 cm sealed polyester bags made from 0.5-mm mesh tissue. The bags were placed horizontally in the 5- to 10-cm layer and covered with the upper 0- to 5-cm layer soil. The experiment lasted from 13 November 1998 to 11 November 2000. For each series, nine samplings (+1 at time 0) were performed, collecting four replicates at each sampling (see Figures 2 and 3 in section 3 for sampling dates).

2.4. Data Acquisition

[8] At sampling, the wet sample was homogenized and 3 × 5 g wet soil was dried at 105°C for the measurement of the moisture content. The remaining wet soil was sub-sampled for analyses of (1) microbial biomass-^{14}C and -^{15}N (four field replicates × two analysis replicates for MB-^{14}C, four field replicates for MB-^{15}N), and (2) total-^{14}C, (four × eight replicates) and -^{15}N (four × two replicates). Microbial biomass was measured according to the fumigation-extraction method of *Brookes et al.* [1985]: 20 g soil, 150 mL 1 mol($^1/_2K_2SO_4$)L^{-1} extractant, ^{14}C measurement on the extracts by liquid scintillation counting (Tricarb 1500, Packard), measurement of N and ^{15}N by Kjeldahl procedure and isotope mass spectrometry (Finnigan delta S), k_{eC} (the microbial biomass-C correcting factor) = 0.45 [*Joergensen*, 1996], and k_{EN} (N correcting factor) = 0.54 [*Joergensen and Mueller*, 1996]. Total C and ^{14}C were measured simultaneously using Carmograph 12A

(Wösthoff, Bochum, Germany), according to *Bottner and Warembourg* [1976]. Total N and ^{15}N were measured using coupled CHN/isotope mass spectrometry.

[9] Climatic parameters (daily precipitation, mean air temperature, and total radiation) were recorded using an automatic Campbell weather station at the site throughout the experiment period.

2.5. Predictive Models

[10] The five models tested with Vensim software (Ventana Systems, Inc., Harvard, Massachusetts) are presented in Figure 1. Three compartments are present in all the models: labile (VL), stable (VS) fractions of necromass (NC = VL + VL) and microbial biomass (MB). MOMOS-3, -4, and -5 contain a compartment for humified compounds (H). MOMOS-2 and -6 contain compartments for labile (HL) and stable (HS) humified compounds. MOMOS-2 is the model already presented by *Sallih and Pansu* [1993] using data from a labeling experiment performed under laboratory conditions, with measurements of total ^{14}C, microbial biomass ^{14}C and not yet decomposed plant fragments ^{14}C. MOMOS-3 results from the simplification of MOMOS-2, with an equation system analogous to the Roth-C model [*Jenkinson*, 1990], but without the inert organic matter compartment of Roth-C (not necessary for this short-term ^{14}C and ^{15}N experiment). MOMOS-4 offers a further simplification of MOMOS-3: The recycling part of H and MB compartments are removed. MOMOS-5 explores two new modifications: (1) the whole outputs from plant material (VL+VS) and humus (H) compartments are the inputs of MB, and (2) the outputs of MB are defined by a respiration quotient (q_{CO2}) and a microbial mortality rate (k_{MB}). The equation system of MOMOS-5 is similar to that of the CANDY model [*Franko et al.*, 1995] and to that used by *Saggar et al.* [1996] to calculate ^{14}C turnover and residence times in soils. However, MOMOS-5 differs from the former models in the following aspects: (1) fractionation of NC inputs into VL and VS, (2) change of kinetic calculation of the microbial respiration (see below, equations (9) and (10)), and (3) elimination of the flow fractionation between necromass and MB used in CANDY (in MOMOS-5 the whole flow from the NC substrate enters into MB). MOMOS-6 attempts to improve MOMOS-5 by introducing a stable humus compartment (HS) that results from the slow maturation of HL and supplies the dormant MB with maintenance energy, when the fresh C input is exhausted. MOMOS-5 and -6 are only regulated by first-order kinetic constants (k parameters, dimension t^{-1}), without the dimensionless parameters (efficiency factors) often used in SOM models to fractionate the flows between the compartments (P parameters in MOMOS-2 to -4, or, e.g., *Jenkinson and Rayner* [1977], *Parton et al.* [1987], or *Franko et al.* [1995]).

[11] For each model, the initial necromass (NC) was partitioned over VL and VR on the basis of its biochemical characteristics using the equations proposed by *Thuriès et al.* [2001, 2002], which give for this labeled straw the stable fraction of NC: $f_s = 0.107$.

[12] The general equation of the models is

$$\dot{\mathbf{x}} = \mathbf{A}\,\mathbf{x}, \tag{1}$$

where $\mathbf{x}$ is the vector of the state variables (compartments), $\dot{\mathbf{x}}$ is the vector of the rates variables, and $\mathbf{A}$ is the parameter matrix of each model. $\mathbf{A}$ and $\mathbf{x}$ are written, for MOMOS-2,

$$\mathbf{A} = \begin{vmatrix} -k_{VL} & 0 & 0 & 0 & 0 \\ 0 & -k_{VS} & 0 & 0 & 0 \\ P_{MB}k_{VL} & P_{MB}k_{VS} & (P_{MB}-1)\,k_{MB} & P_{MB}k_{HL} & P_{MB}k_{HS} \\ P_{HL}k_{VL} & P_{HL}k_{VS} & P_{HL}k_{MB} & (P_{HL}-1)\,k_{HL} & P_{HL}k_{HS} \\ P_{HS}k_{VL} & P_{HS}k_{VS} & P_{HS}k_{MB} & P_{HS}k_{HL} & (P_{HS}-1)\,k_{HS} \end{vmatrix}$$

$$\mathbf{x} = \begin{vmatrix} VL \\ VS \\ MB \\ HL \\ HS \end{vmatrix}, \tag{2}$$

for MOMOS-3,

$$\mathbf{A} = \begin{vmatrix} -k_{VL} & 0 & 0 & 0 \\ 0 & -k_{VS} & 0 & 0 \\ P_{MB}k_{VL} & P_{MB}k_{VS} & (P_{MB}-1)k_{MB} & P_{MB}k_{H} \\ P_{H}k_{VL} & P_{H}k_{VS} & P_{H}k_{MB} & (P_{H}-1)k_{H} \end{vmatrix}$$

$$\mathbf{x} = \begin{vmatrix} VL \\ VS \\ MB \\ H \end{vmatrix}, \tag{3}$$

for MOMOS-4,

$$\mathbf{A} = \begin{vmatrix} -k_{VL} & 0 & 0 & 0 \\ 0 & -k_{VS} & 0 & 0 \\ P_{MB}k_{VL} & P_{MB}k_{VS} & -k_{MB} & 0 \\ P_{H}k_{VL} & P_{H}k_{VS} & 0 & -k_{H} \end{vmatrix} \qquad \mathbf{x} = \begin{vmatrix} VL \\ VS \\ MB \\ H \end{vmatrix}, \tag{4}$$

for MOMOS-5,

$$\mathbf{A} = \begin{vmatrix} -k_{VL} & 0 & 0 & 0 \\ 0 & -k_{VS} & 0 & 0 \\ k_{VL} & k_{VS} & -(q_{CO_2}+k_{MB}) & k_{H} \\ 0 & 0 & k_{MB} & -k_{H} \end{vmatrix} \qquad \mathbf{x} = \begin{vmatrix} VL \\ VS \\ MB \\ H \end{vmatrix}, \tag{5}$$

and for MOMOS-6,

$$\mathbf{A} = \begin{vmatrix} -k_{VL} & 0 & 0 & 0 & 0 \\ 0 & -k_{VS} & 0 & 0 & 0 \\ k_{VL} & k_{VS} & -(q_{CO_2}+k_{MB}) & k_{HL} & k_{HS} \\ 0 & 0 & k_{MB} & -(k_{HL}+k_{HLS}) & 0 \\ 0 & 0 & 0 & k_{HLS} & -k_{HS} \end{vmatrix}$$

$$\mathbf{x} = \begin{vmatrix} VL \\ VS \\ MB \\ HL \\ HS \end{vmatrix}, \tag{6}$$

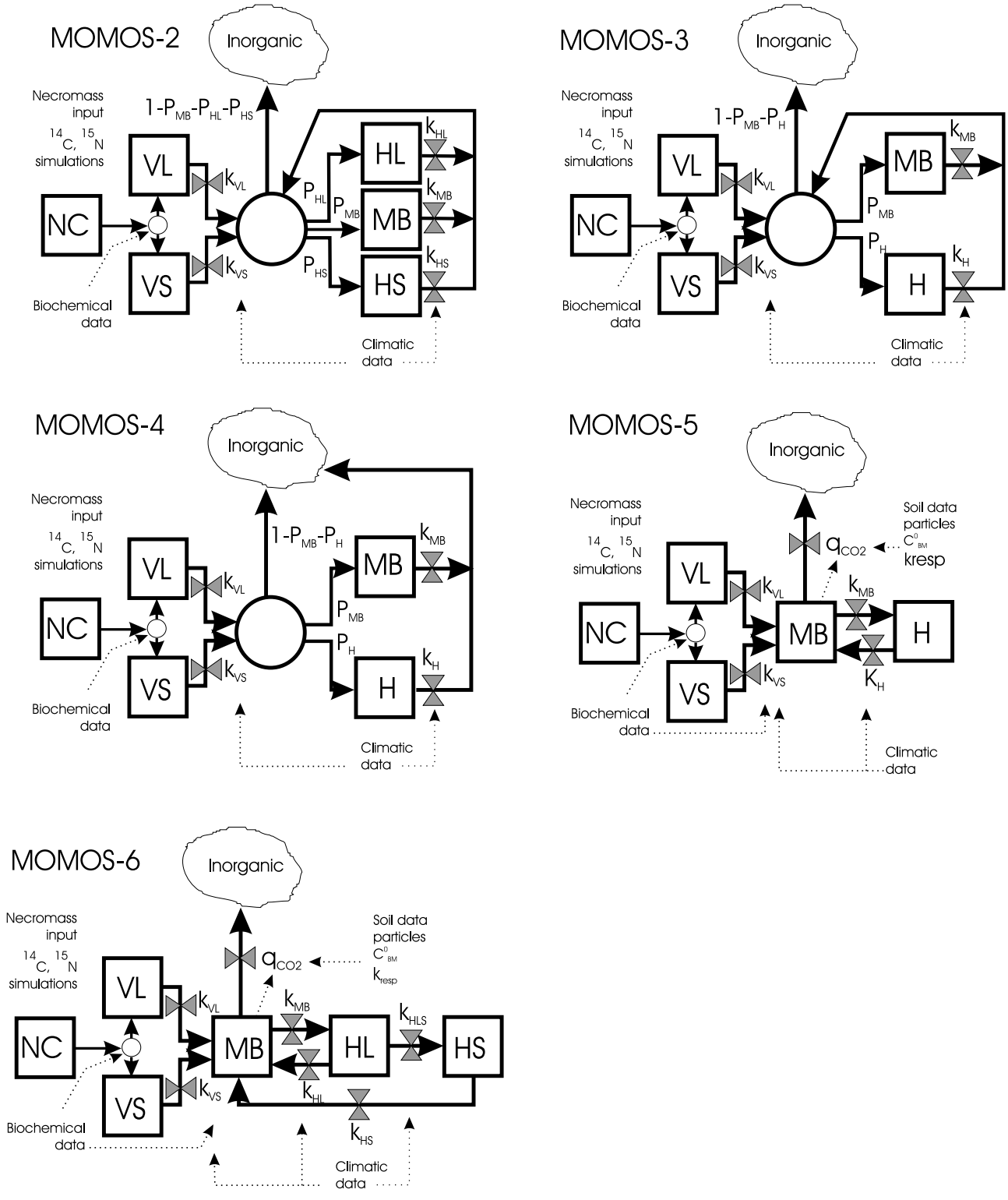

Figure 1. Flow diagram's of the five versions of the MOMOS model compared. NC, total necromass; VL, labile necromass; VS, stable necromass; MB, microbial biomass; H, humified compounds (humus); HL, labile humus; HS, stable humus.

For the labeling experiment described in this paper (one single initial input of dead matter and an initial amount C_0 of ^{14}C with a stable fraction f_S), the initial conditions are given by

$$\begin{aligned} VL(0) &= (1 - f_S)C_0, \\ VS(0) &= f_S\, C_0, \\ MB(0) &= 0, \\ H(0) &= 0, \\ HL(0) &= 0, \\ HS(0) &= 0, \\ CO_2(0) &= 0. \end{aligned} \tag{7}$$

[13] At each incubation time, the total ^{14}C evolution $\dot{c}$ from the n compartments ($n = 4$ for MOMOS-3, -4, -5; $n = 5$ for MOMOS-2, -6) is given by

$$\dot{c} = \sum_{i=1}^{n} \dot{x}_i \qquad c(0) = C_0. \tag{8}$$

[14] In the case of MOMOS-5 and -6, equation (8) becomes particularly simple,

$$\dot{c} = -q_{CO2}\ MB, \tag{9}$$

where q_{CO2} is the metabolic quotient of the microbial biomass [*Anderson and Domsch*, 1993]. Another condition is necessary to ensure correct performance of MOMOS-5 and -6: q_{CO2} must be controlled by the amount of MB. The q_{CO2} increases when MB is growing (particularly in response to the initial high supply from VL) and decreases when MB decreases or becomes inactive (dormant MB). Then $\dot{c}$ is linked to MB by a second-order kinetics. In order to allow use of MOMOS-5 or -6 in different situations, we suggest (1) the introduction of a respiratory coefficient k_{resp} (dimension t^{-1}) and (2) the weighting of the k_{resp} values by the ratio of the actual level of MB in the studied soil and its equilibrium value (C^0_{MB} measured in biologically stable soil, i.e., a long time after the former inputs of substrate). For the present labeling experiment, $C^0_{MB} = 0.15$ g kg^{-1}, the level of MB-^{14}C measured at the end of the experiment. The q_{CO2} is given by

$$q_{CO2} = k_{resp} \frac{MB}{C^0_{MB}}. \tag{10}$$

[15] The N calculation of MOMOS-2 to -6 is simplified compared to the initial MOMOS-N model (MOMOS-1 [*Pansu et al.*, 1998]). Ammonia and nitrate pools are combined in a single pool of inorganic-N. For each of the five models, the N state variables are derived from the C model, using the C-to-N ratios of the compartments. If $\boldsymbol{\eta}$ is the vector of the C-to-N ratios and $\mathbf{y}$ is the vector of N contents, the simulation of organic N status at a given incubation time is governed by

$$\mathbf{y} = \frac{\mathbf{x}}{\boldsymbol{\eta}}. \tag{11}$$

If η_0 is the initial ^{14}C-to-^{15}N ratio of the plant material, the inorganic ^{15}N (iN) is

$$iN = \frac{C_0}{\eta_0} - \sum_{i=1}^{n} y_i. \tag{12}$$

In this labeling experiment, the values η_0, η_t (remaining total ^{14}C-to- remaining total ^{15}N), and η_{MB} (^{14}C-to-^{15}N of microbial biomass) were measured. The η_{VL} value is linked to η_0 and η_{VS} by

$$\eta_{VL} = \frac{(1 - f_S)}{\left(\frac{1}{\eta_0} - \frac{f_S}{\eta_{VS}}\right)}. \tag{13}$$

The η_H or η_{HL} values are linked to the other data by

$$\eta_H = \frac{x_H}{\frac{C_t}{\eta_t} - \frac{x_{VL}}{\eta_{VL}} - \frac{x_{VS}}{\eta_{VS}} - \frac{x_{MB}}{\eta_{MB}}} \tag{14}$$

$$\eta_{HL} = \frac{x_{HL}}{\frac{C_t}{\eta_t} - \frac{x_{VL}}{\eta_{VL}} - \frac{x_{VS}}{\eta_{VS}} - \frac{x_{MB}}{\eta_{MB}} - \frac{x_{HS}}{\eta_{HS}}}. \tag{15}$$

Thus the only η values that have to be estimated are η_{VS} (^{14}C-to-^{15}N of the stable fraction of NC) in MOMOS-3 to -5 or η_{VS} and η_{HS} (^{14}C-to-^{15}N of the stable fraction of humus) in MOMOS-2 and -6. In order to avoid irregularities in predictions, the values calculated for η_H or η_{HL} are smoothed in the interval $[\eta_{MB}, \frac{2}{5}(\eta_0 + \eta_{MB})]$ with $\eta_{HS} = 6\ \eta_{MB}/5$ for MOMOS-6.

[16] During the simulations, the kinetic constants are daily corrected by two functions, one for temperature $f(T)$ and one for moisture $f(w)$; $f(T)$ is a law with Q10 = 2 for a reference temperature of 20°C assumed to be valid for these mountain soils [*Kätterer et al.*, 1998]; $f(w)$ is a linear function of the actual soil moisture scaled by moisture content at field capacity ($f(w) = 0$ for $w = 0$). For the 5- to 10-cm soil layer, the actual moisture was calculated by the SAHEL model [*Penning de Vries et al.*, 1989]. With the corrective factor $f(T) \times f(w)$ in [0, 1] interval, the general formulation (equation (1)) of the models becomes

$$\dot{\boldsymbol{x}} = f(T)f(w)\mathbf{A}\ \mathbf{x}. \tag{16}$$

2.6. Comparison of the Predictive Quality and Sensitivity of the Models

[17] The four vectors of measured data were:

- $\mathbf{x}_t$ = total ^{14}C (nine sampling occasions (so) during 2 years of incubation), corresponding to the predicted values $\hat{\mathbf{x}}_t = \sum_{i=1}^{n} \mathbf{x}_i$,

Table 1. Estimated Values of the Parameters for the Five Tested Models[a]

	Parameter Values												
Model	k_{VL}	k_{VS}	k_{MB}	k_{HL}	k_H	$k_{HS,,}$	k_{HLS}	k_{resp}	P_{MB}	P_H	P_{HS}	η_{VS}	η_H	η_{HS}
MOMOS-2	0.54	0.004	0.01	k_{VL}		k_{VS}			0.014		0.08	500		10.5
MOMOS-3	0.13	0.004	0.01		k_{VS}				0.06	0.36		450	10.9	
MOMOS-4	0.13	0.002	0.007		k_{VS}				0.06	0.36		500	10.5	
MOMOS-5	0.6	0.003	0.45		0.05			0.03				27	Cal	
MOMOS-6	0.6	0.003	0.45	0.05		$5\ 10^{-5}$	$3\ 10^{-4}$	0.03				46	Cal	9.9
	Sensitivity Analysis (S_{sv}, Equation (19)) of MOMOS-4 (Type 1) Model													
SV	k_{VL}	k_{VS}	k_{MB}	k_{HL}	k_H	$k_{HS,,}$	k_{HLS}	k_{resp}	P_{MB}	P_H	P_{HS}	η_{VS}	η_H	η_{HS}
Tot-^{14}C 3 m	0.17	0.17	0.05		0.17				0.17	1.5				
Tot-^{14}C 24 m	0.03	1.0	0.14		1.0				0.09	1.7				
Tot-^{15}N 3 m	0.04	0.09	0.05		0.09				0.27	1.9				
Tot-^{15}N 24 m	0.03	0.9	0.2		0.9				0.14	2				
MB-^{14}C 3 m	0.17	0.08	0.3		0.08				2.5	0				
MB-^{14}C 24 m	0.07	0.15	3.2		0.15				2.4	0				
MB-^{15}N 3 m	0.16	0.07	0.2		0.07				2.4	0				
MB-^{15}N 24 m	0.05	0.12	3.8		0.12				2.3	0				
	Sensitivity Analysis (S_{sv}, Equation (19)) of MOMOS-6 (type 2) Model													
SV	k_{VL}	k_{VS}	k_{MB}	k_{HL}	k_H	$k_{HS,,}$	k_{HLS}	k_{resp}	P_{MB}	P_H	P_{HS}	η_{VS}	η_H	η_{HS}
Tot-^{14}C 3 m	0.3	0.02	1.2	0.5		<0.01	0.01	0.7						
Tot-^{14}C 24 m	0.2	0.16	2.3	2.0		<0.01	0.16	1.1						
Tot-^{15}N 3 m	0.4	0.02	1.2	0.5		<0.01	0.01	0.9						
Tot-^{15}N 24 m	0.2	0.16	2.2	2.0		<0.01	0.2	1.2						
MB-^{14}C 3 m	0.4	0.04	0.20	1.4		<0.01	0.02	1.1						
MB-^{14}C 24 m	0.2	0.15	0.43	0.43		<0.01	0.09	1.5						
MB-^{15}N 3 m	0.4	0.04	0.35	1.4		<0.01	0.02	1.1						
MB-^{15}N 24 m	0.3	0.09	0.56	0.56		<0.01	0.06	1.5						

[a]Abbreviations: k, first-order kinetic constants (day^{-1}); P, fraction of flow (dimensionless); η, estimated ^{14}C-to-^{15}N ratio. Sensitivity analysis to parameter fluctuations of the four-state variable Total-^{14}C, Total-^{15}N, MB-^{14}C, and MB-^{15}N is at 3 and 24 m of incubation.

$-\mathbf{y}_t$ = total ^{15}N (nine so) corresponding to the predicted values $\hat{\mathbf{y}}_t = \sum_{i=1}^{n} \mathbf{y}_i$,

$-\mathbf{x}_{MB}$ = MB-^{14}C (nine so) corresponding to the predicted values $\hat{\mathbf{x}}_{MB}$,

$-\mathbf{y}_{MB}$ = MB-^{15}N (nine so) corresponding to the predicted values $\hat{\mathbf{y}}_{MB}$,

For each model, four residual sums of square (RSS) were calculated for the m so,

$$\begin{aligned} RSS_{xt} &= \sum_{j=1}^{m} (\mathbf{x}_t - \hat{\mathbf{x}}_t)^2, \\ RSS_{yt} &= \sum_{j=1}^{m} (\mathbf{y}_t - \hat{\mathbf{y}}_t)^2, \\ RSS_{xMB} &= \sum_{j=1}^{m} (\mathbf{x}_{MB} - \hat{\mathbf{x}}_{MB})^2, \\ RSS_{yMB} &= \sum_{j=1}^{m} (\mathbf{y}_{MB} - \hat{\mathbf{y}}_{MB})^2. \end{aligned} \tag{17}$$

[22] The smallest RSS corresponds to the best fit. In addition, the comparison should take the number of model parameters p into account. The best model has the smallest RSS and also the smallest p. MOMOS-5 has five parameters: k_{VL}, k_{VS}, k_{MB}, k_{HL}, and k_{resp}. MOMOS-3 and -4 have six parameters: k_{VL}, k_{VS}, k_{MB}, k_H, P_{MB}, and P_H. However, the specific parameterization of this experiment takes $k_{VS} = k_H$ and reduces MOMOS-3 and -4 to five parameter models. MOMOS-2 has eight parameters: k_{VL}, k_{VS}, k_{HL}, k_{HS}, k_{MB}, P_{HL}, P_{MB}, and P_{HS}. However, again, the parameterization of this experiment takes $k_{VL} = k_{HL}$, $k_{VS} = k_{HS}$, and $P_{HL} = 0.77$ (value found by *Sallih and Pansu* [1993]) and also reduces MOMOS-2 to a five-parameter model.

[23] Thus the predictive quality of the models MOMOS-2−-5 can be pairwise compared by the F tests,

$$F_{(m-1,m-1)} = \begin{cases} RSS_{MOMOS-t}/RSS_{MOMOS-u} & \text{if } RSS_{MOMOS-t} > RSS_{MOMOS-u} \\ RSS_{MOMOS-u}/RSS_{MOMOS-t} & \text{if } RSS_{MOMOS-u} > RSS_{MOMOS-t} \end{cases}, \tag{18}$$

(u, $t \in [2-5]$, $t \neq u$, m sampling occasions, for each of the four models applied to each of the four series total-^{14}C and -^{15}N, MB-^{14}C, and -^{15}N.

[24] For a given state variable (SV), a scaled dimensionless sensitivity to a parameter (PA) can be defined by

$$S_{SV} = \frac{\Delta_{SV}\ SV^{-1}}{\Delta_{PA}\ PA^{-1}} \tag{19}$$

for the SV total-^{14}C, total-^{15}N, MB-^{14}C, and MB-^{15}N from 13 November 1998 to 11 November 2000 at a daily time step. The values of the parameters were randomly sampled (200 simulations) from a normal distribution. For each parameter, the mean of the distribution is presented in Table 1; the relative standard deviation (sd) was 10%.

3. Results

3.1. Parameters and Sensitivity of the Models

[25] Since there was no significant difference between the results from series F2y and F7y, all the predictions for each

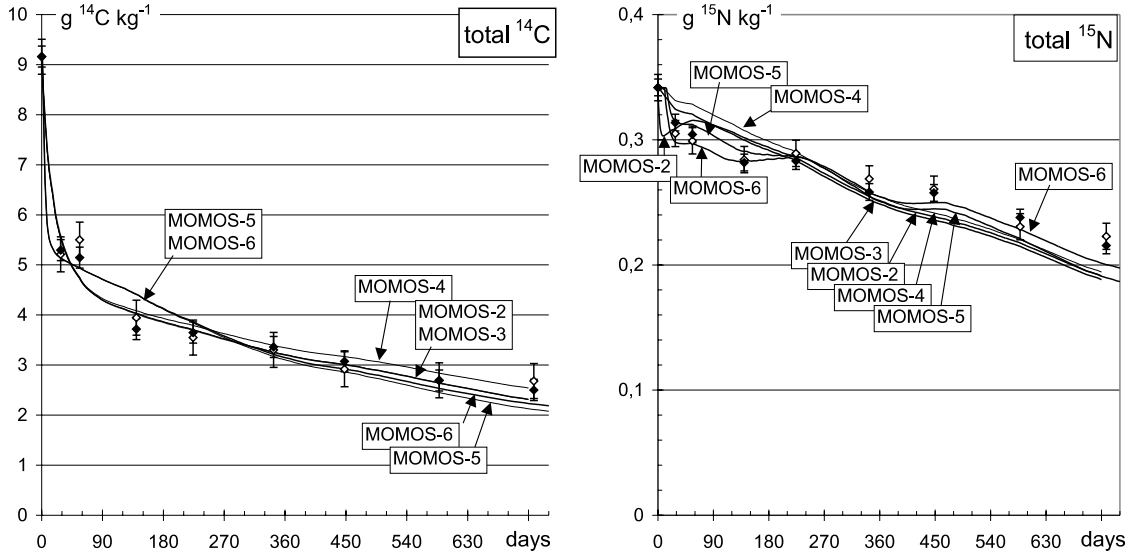

Figure 2. Model predictions (lines) and measured data of total-^{14}C and -^{15}N for the two series (solid diamonds, F2y; open diamonds, F7y) with pooled 95% confidence interval (nine sampling occasions × four field replicates × two to eight analysis replicates). Day 0 is 13 November 1998.

model are based on only one set of parameters (the mean value from F2y and F7y calculations, Table 1). The results of sensitivity analysis of the five models show (1) a similar behavior of MOMOS-2 to -4 and (2) a similar behavior of MOMOS-5 and -6. Therefore MOMOS-4 was chosen in Table 1 as being representative of MOMOS-2 to -4 (type 1 models), and MOMOS-6 was chosen as being representative of the type 2 models. Type 1 defines models with two types of parameters: kinetic constants and flow fractionation (efficiency factors). Type 2 defines models with only kinetic constants as parameters; consequently, all the parameters of type 2 models are linked to climatic variations.

3.2. Total ^{14}C and ^{15}N Predictions

[26] The predictions of the five models and the measured F2y and F7y values are plotted in Figure 2. Tables 2 and 3 compare the predictive quality (equation (18)) of the models for total ^{14}C and ^{15}N, respectively.

[27] For total ^{14}C, the MOMOS-2 and MOMOS-3 predictions were almost identical. For the other models the predictions were slightly different (Figure 2), but all the results were statistically equivalent (Table 2). The MOMOS-5 and -6 predictions were also almost identical during the first 9 months, as long as the HS content (MOMOS-6) was low. At the end of the experiment, MOMOS-6 predicted slightly higher values, closer to the measured data than MOMOS-5, indicating a ^{14}C-sequestration in the HS compartment.

[28] For total ^{15}N predictions, slight differences appeared between the models (Figure 2), but they were again all statistically equivalent (Table 3). The MOMOS-2 to -4 predictions were overestimated during the first 6 months of incubation and underestimated during the last year. The MOMOS-5 and especially the MOMOS-6 predictions were the closest to the measured values throughout the whole incubation period. The slight underestimation observed during the last year could be explained by a slight overestimation of the measured ^{15}N; total-^{15}N is defined in MOMOS as organic-^{15}N, whereas the measurements include small amounts of inorganic ^{15}N remaining in the soil.

[29] The sensitivity analysis (Table 1) shows that the total ^{14}C and total ^{15}N predicted by the type 1 models are mainly influenced by the P_H values, that is, the fraction of materials transformed in stable humus. In type 2 models, the effect of the parameters fluctuation on total ^{14}C and total ^{15}N predictions is better balanced. The most active parameters are the mortality constant of MB (k_{MB}), the respiration constant of MB (k_{resp}), the MB input from HL (K_{HL}),

Table 2. *F* Tests (Equation (18)) Applied to the Comparison of the Residual Sums of Squares (RSS) of Total ^{14}C Predictions for the Two Data Series F2y and F7y[a]

	MOMOS-3		MOMOS-4		MOMOS-5		MOMOS-6	
Model	F2y	F7y	F2y	F7y	F2y	F7y	F2y	F7y
MOMOS-2	$1.00^{2,\ NS}$	$1.13^{2,\ NS}$	$1.06^{2,\ NS}$	$1.10^{2,\ NS}$	$2.17^{2,\ NS}$	$1.16^{2,\ NS}$	$1.83^{2,\ NS}$	$1.00^{6,\ NS}$
MOMOS-3			$1.06^{3,\ NS}$	$1.02^{4,\ NS}$	$2.16^{3,\ NS}$	$1.02^{3,\ NS}$	$1.83^{3,\ NS}$	$1.13^{6,\ NS}$
MOMOS-4					$2.05^{4,\ NS}$	$1.05^{4,\ NS}$	$1.73^{4,\ NS}$	$1.10^{6,\ NS}$
MOMOS-5							$1.18^{6,\ NS}$	$1.16^{6,\ NS}$

[a]Exponent close to *F* value is MOMOS number with the smallest RSS; NS denotes not significant.

Table 3. F Tests (Equation (18)) Applied to the Comparison of the Residual Sums of Squares (RSS) of Total ^{15}N Predictions for the Two Data Series F2y and F7y[a]

	MOMOS-3		MOMOS-4		MOMOS-5		MOMOS-6	
Model	F2y	F7y	F2y	F7y	F2y	F7y	F2y	F7y
MOMOS-2	$1.34^{2,\ NS}$	$1.36^{2,\ NS}$	$1.36^{2,\ NS}$	$1.38^{2,\ NS}$	$1.28^{2,\ NS}$	$1.14^{5,\ NS}$	$1.74^{6,\ NS}$	$1.53^{6,\ NS}$
MOMOS-3			$1.02^{3,\ NS}$	$1.01^{3,\ NS}$	$1.04^{5,\ NS}$	$1.77^{5,\ NS}$	$1.81^{6,\ NS}$	$2.09^{6,\ NS}$
MOMOS-4					$1.06^{5,\ NS}$	$1.79^{5,\ NS}$	$1.85^{6,\ NS}$	4.35^{6}
MOMOS-5-s							$1.74^{6,\ NS}$	$2.43^{6,\ NS}$

[a]Exponent close to F value is MOMOS number with the smallest RSS; NS denotes not significant.

especially at the end of incubation, and the MB input from VL (k_{VL}), especially at 3 months of incubation.

3.3. Predictions of MB-^{14}C and -^{15}N

[30] The predicted and measured values of MB in the F2y and F7y series are plotted in Figure 3. Tables 4 and 5 compare the predictive quality (equation (18)) of the models for MB-^{14}C and -^{15}N, respectively. The MOMOS-2 and -3 predictions were almost identical and were close to the MOMOS-4 predictions. In all cases the results show clearly a significant improvement of the MB predictions by MOMOS-5 compared to those by MOMOS-2 to -4. For MB-^{14}C, the improvement was significant at 5% risk in five cases and at 2% risk in one case. For MB-^{15}N, the improvement was significant at 10% risk in two cases and at 5% in the four other cases. During the first 5 months the MOMOS-5 and -6 predictions were again similar. After this time the MOMOS-6 predictions were slightly closer to the measured values of MB-^{14}C and -^{15}N.

[31] The sensitivity analysis (Table 1) shows that MB-^{14}C and MB-^{15}N predicted by the type 1 models are mostly controlled by the P_{MB} values (the fraction of materials transformed in microbial biomass) during the whole incubation period. At the end of experiment, these MB-^{14}C and MB-^{15}N predictions are also very sensitive to k_{MB} values (the kinetic constant of the MB output), but during the whole incubation the predictions do not depend on the P_H value; symmetrically, the H-^{14}C and H-^{15}N predictions do not depend on the P_{MB} values. The MB-^{14}C and MB-^{15}N predictions are more stable in type 2 than in type 1 models: The maximum S_{SV} value is 2.5 in type 1 models and 1.5 in type 2 models (Table 1). These predictions are most sensitive to the k_{resp} values (the respiratory coefficient of MB) and, second, at the beginning of incubation, to the k_{HL} (the input into MB from HL) and k_{VL} (the input into MB from VL) values.

4. Discussion

4.1. Comparison of MOMOS-2 and MOMOS-3

[32] MOMOS-3 differs from MOMOS-2 by the absence of the labile humus compartment (HL, Figure 1). This results in very different values of the first-order kinetic constants of VL: $k_{VL} = 0.54$ ($t^{1/2} = 1.3$ days) for MOMOS-2 and $k_{VL} = 0.13$ ($t^{1/2} = 5.3$ days) for MOMOS-3 (Table 1). In MOMOS-2 the labile metabolites are subsequently transferred to the transient HL compartment. The predictions of the two models are similar for total-^{14}C and MB-^{14}C, as

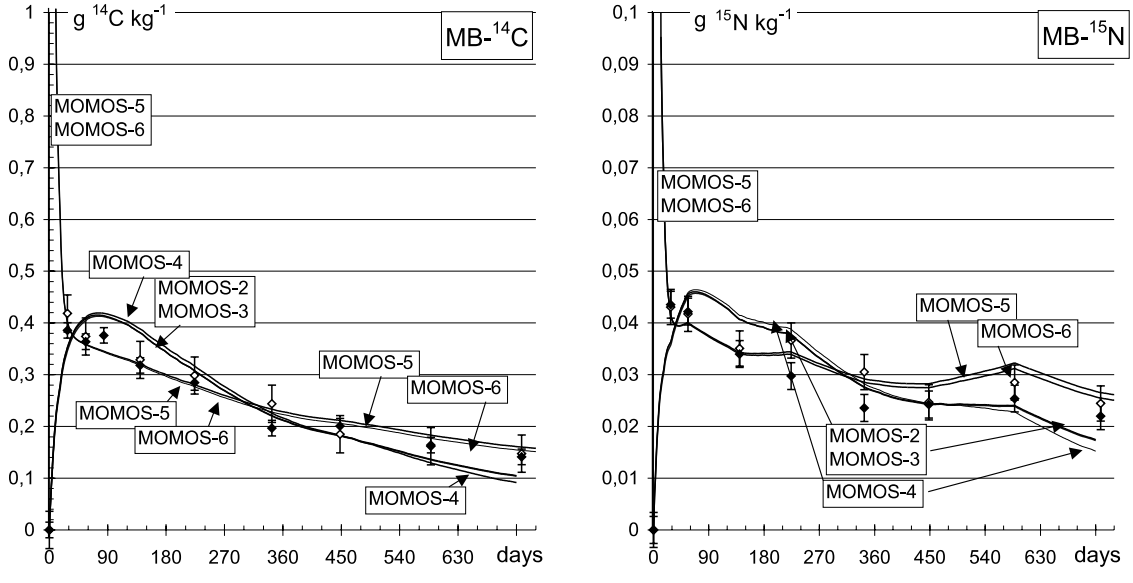

Figure 3. Model predictions (lines) and measured data of MB-^{14}C and -^{15}N for the two series (solid diamonds, F2y; open diamonds, F7y) with pooled 95% confidence interval (nine sampling occasions × four field replicates). Day 0 is 13 November 1998.

Table 4. *F* Tests (Equation (18)) Applied to the Comparison of the Residual Sums of Squares (RSS) of MB-^{14}C Predictions for the Two Data Series F2y and F7y[a]

	MOMOS-3		MOMOS-4		MOMOS-5		MOMOS-6	
Model	F2y	F7y	F2y	F7y	F2y	F7y	F2y	F7y
MOMOS-2	$1.02^{3,\ NS}$	$1.09^{3,\ NS}$	$1.31^{2,\ NS}$	$1.20^{2,\ NS}$	$4.51^{5,\ A}$	$5.22^{5,\ A}$	6.60^{6}	5.80^{6}
MOMOS-3			$1.33^{3,\ NS}$	$1.22^{3,\ NS}$	$4.43^{5,\ A}$	$5.12^{5,\ A}$	6.48^{6}	5.69^{6}
MOMOS-4					$5.88^{5,\ A}$	$6.26^{5,\ B}$	8.61^{6}	6.97^{6}
MOMOS-5							1.46^{6}	1.11^{6}

[a]Exponent close to *F* value is MOMOS number with the smallest RSS; A, B, and NS denote RSS significant difference at 5% and 2% risk and not significant, respectively.

well as for MB-^{15}N (Figures 2 and 3). The slight but not significant differences observed for total-^{15}N resulted from the estimated C-to-N ratio (equation (15)) of the HL compartment. Thus the two models are clearly equivalent in predicting the total SOM dynamics. The MOMOS-2 decay rate of HL and VL are identical ($k_{HL} = k_{VL}$). Both VL and HL compartments are quickly and almost completely exhausted after 90–120 days of incubation; at that time, MB reaches its maximum values and begins also to decline; this highlights the role of labile compounds in the MB dynamics. In MOMOS-3, the VL compartment represents the sum VL + HL of MOMOS-2 and is exhausted at the same time. Thus MOMOS-3, with an equation system analogous to the Roth-C model [*Jenkinson*, 1990], is a valuable simplification of MOMOS-2. Nevertheless, the need of the HL compartment was supported from another labeling experiment [*Sallih and Pansu*, 1993] performed under controlled laboratory conditions where, in addition to the MB measurement, the not yet decomposed plant fragments-^{14}C (NC) remaining in the soil were also measured: HL-^{14}C = total-^{14}C minus (MB-^{14}C + plant fragments-^{14}C). The HL compartment describes a real transient decomposition step. Nevertheless, in modeling the total C and N dynamics from long field experiments with this type of model, HL can be eliminated. Thus MOMOS-3, with an equation system analogous to the Roth-C model [*Jenkinson*, 1990], is a valuable simplification of MOMOS-2.

4.2. Comparison of MOMOS-3 and MOMOS-4

[33] MOMOS-4 is a further simplification derived from MOMOS-3 by suppressing the recycling loop of MB and H outputs (Figure 1). MOMOS-4 is a parallel decomposition model in which a part P_{MB} of the flow from VL and VS becomes MB and another part P_H becomes H. In the mathematical description of MOMOS-4, this simplification eliminates the *P* parameters from the diagonal terms (see matrix equation (3)). In the matrix of equation (4), the diagonal terms become first-order kinetic constants; all the terms above the diagonal become zero. The calculated MOMOS-3 and -4 parameters are similar, except the slightly lower first-order kinetic constants k_{VS} (and $k_H = K_{VS}$) and k_{MB} in MOMOS-4. This is in accordance with the removal of the recycling part in MOMOS-4.

[34] In Tables 3, 4, and 5, RSS-3 was always lower than RSS-4, indicating a tendency of more accurate predictions for MOMOS-3 than for MOMOS-4, but the differences were never significant. Given the RSS ratios (Tables 2–5), the models 3 and 4 predictions are never significantly different. Consequently, MOMOS-4 is preferable because of its simpler structure.

4.3. Comparison of MOMOS-4 (Type 1 Models) and MOMOS-5 (Type 2)

[35] In MOMOS-5, the estimated first-order kinetic constant k_{VL} is higher than in MOMOS-3 and -4 and close to the MOMOS-2 value (Table 1). However, in MOMOS-5, the VL labile plant material is entirely assimilated by MB, while in MOMOS-2, VL becomes, for the P_{HL} part, labile humus (HL). Consequently, MOMOS-5 and MOMOS-2 to -4 generate different MB curves. In MOMOS-5, the predicted MB increased sharply during the 3 initial days, reaching for MB-^{14}C 20 to 30% of Total-^{14}C, and for MB-^{15}N over 80% of Total-^{15}N for all treatments (not shown in Figure 3). After this initial quick peak, MB-^{14}C and -^{15}N decreased rapidly, giving significantly better predictions than MOMOS-2 to -4 from day 30 until the end of the incubation.

[36] In this experiment, the first measurement occurred at day 30, i.e., at the end of the MB initial peak (Figure 3). The shape of the MOMOS-5 MB curve agrees with literature data: The response time of MB to the addition of labile organic substrate is generally on the order from a few hours

Table 5. *F* Tests (Equation (18)) Applied to the Comparison of the Residual Sums of Squares (RSS) of MB-^{15}N Predictions for the Two Data Series F2y and F7y[a]

	MOMOS-3		MOMOS-4		MOMOS-5-s		MOMOS-5	
Model	F2y	F7y	F2y	F7y	F2y	F7y	F2y	F7y
MOMOS-2	1.02^{NS}	$1.09^{3,\ NS}$	$1.36^{2,\ NS}$	$1.22^{2,\ NS}$	$3.94^{5,\ A}$	$4.46^{5,\ B}$	6.23^{6}	5.70^{6}
MOMOS-3			$1.39^{3,\ NS}$	$1.33^{3,\ NS}$	$3.85^{5,\ A}$	$4.07^{5,\ B}$	6.08^{6}	5.21^{6}
MOMOS-4					$5.35^{5,\ B}$	$5.42^{5,\ B}$	8.46^{6}	6.93^{6}
MOMOS-5-s							1.58^{6}	1.28^{6}

[a]Exponent close to *F* value is MOMOS number with the smallest RSS; A, B, and NS denote RSS significant difference at 10% and 5% risk and not significant, respectively.

[*Anderson and Domsch*, 1978] to a few days. The maximum size of MB is often observed at the first measurement, i.e., about 7–10 days after the substrate addition [*Henriksen and Breland*, 1999; *Lundquist et al.*, 1999; *Ocio et al.*, 1991; *Trinsoutrot et al.*, 2000]. An immediate N microbial immobilization was measured from the beginning of the incubation using various substrates by *Pansu and Thuriès* [2003], *Pansu et al.* [2003], and *Trinsoutrot et al.* [2000]. Conversely, for MOMOS-2 to -4, the predicted MB curve increases slowly, reaching the maximum level only after about 2 months of incubation. Thus MOMOS-2 to -4 underestimate MB at the first measurements, overestimate it during the following few months, and again underestimate it during the second year. A similar discrepancy between the predicted and measured MB has already been observed by *Sallih and Pansu* [1993], using the MOMOS-1 model. Despite the more complex equation describing MB dynamics in type 2 models as compared to type 1, the sensitivity analysis shows a greater stability in type 2 than in type 1 models for MB-^{14}C and -^{15}N predictions. The responses are also more consistent with the ecological definition of the parameters in type 2 than in type 1 models. In type 1, the productions of MB and H are independent (they depend mainly on P_{MB} and P_H, respectively); the two compartments run in parallel without interaction. The type 2 models show a more coherent link between compartments; the total-C and -N and MB-C and -N are better equilibrated in response to the fluctuations of the most acting parameters of the model.

[37] In MOMOS-5 the H compartment has the same input (k_{MB}) and output (k_H) kinetic constants as HL in MOMOS-6. Indeed, H and HL represent labile metabolites, like HL in MOMOS-2. However, H and HL should be interpreted differently. As used in MOMOS-2, HL consists of labile metabolites resulting from decomposing plant material. In MOMOS-5, H consists of metabolites resulting from microbial cadavers or byproducts of microbial activity. Both materials are used (for MOMOS-2 HL) or reused (for MOMOS-5 H) as substrates for microorganisms, but HL in MOMOS-2 is rapidly used and exhausted ($k_{HL} = k_{VL} = 0.54$ day^{-1}), explaining the above-mentioned failures in MB predictions. In contrast, H in MOMOS-5 represents a large reserve of ^{14}C and ^{15}N that persists for the whole incubation period ($k_H = 0.05$ day^{-1}) and sustains the relatively high level of MB until the end of the experiment. This agrees with the conclusions of *Mueller et al.* [1998]: "a part of the decomposed plant material is immobilized both in soil MB as well as in a considerable amount of microbial residual products."

4.4. Improvement of MOMOS-5 by MOMOS-6

[38] MOMOS-6, which results from the improvement of MOMOS-5 by adding a stable humus compartment (HS, Figure 1), shows a tendency toward better RSS for all predicted variables (Tables 2–5). However, MOMOS-6 needs two additional parameters (k_{HLS} and k_{HS}), and the improvement in terms of RSS over MOMOS-5 is not significant. Thus, for the ^{14}C and ^{15}N experiment presented here, the largest improvement in predictive quality is achieved by MOMOS-5. However, the simulation of the dynamics of soil native total-C and -N including slow sequestration and accumulation of C with a long turnover time (work in preparation) required the introduction of the stable humus compartment. In this 2-year experiment, MOMOS-6 predicted an amount of stabilized HS-^{14}C = 0.18 g kg^{-1}, i.e., 2.0% of the total added ^{14}C, and an amount of stabilized HS-^{15}N = 0.018 g kg^{-1}, i.e., 5.4% of added ^{15}N. The HS compartment is also the most important reservoir of stable soil native N.

[39] Figures 2 and 3 show the ecological consistency of the MOMOS-6 improvement. During the second year of incubation, the MOMOS-6 predictions were closer to the measured data than the MOMOS-5 ones. For MB-^{14}C and -^{15}N, the MOMOS-6 predictions were lower than the MOMOS-5 ones, as a response to stabilization in HS. During the same time, total-^{14}C and -^{15}N predictions were higher in MOMOS-6 than in MOMOS-5, logically reflecting a lower microbial mineralization. In contrast, the MOMOS-2 to -4 predictions were less consistent, because lower total-^{14}C values also corresponded to lower MB-^{14}C values (fraction P_{MB}) and vice versa.

5. Conclusions and Recommendations

[40] The five-compartment MOMOS-2 model was initially developed on the basis of a laboratory labeling experiment in which most of the predicted compartments were measured [*Sallih and Pansu*, 1993]. In the present field experiment, under natural climate conditions, with less intensive sampling and a simpler procedure of chemical analysis, the aim was to test the predictive quality and sensitivity of successively simpler versions. The first step was to reduce the number of compartments (MOMOS-2 to -3) and to suppress a recycling process (MOMOS-3 to -4). The successive simplifications did not significantly modify the prediction accuracy for total ^{14}C and ^{15}N, nor for microbial biomass. Thus the simplification of MOMOS-2 to -3 is considered to be valid, as is the further simplification of MOMOS-3 to MOMOS-4. The second step focused on the processes associated with the microbial activity as a key stone compartment. It allowed elimination of the dimensionless parameters used for flow partitioning. As a result, MOMOS-5 only uses (1) the three first-order kinetic constants k_{VL}, k_{VS}, and k_H, which control the inputs into MB, (2) the first-order kinetic constant k_{MB}, which defines the production of microbial cadavers and metabolites, and (3) the metabolic quotient q_{CO2}, which regulates MB respiration. The modifications leading to MOMOS-5 did not change the accuracy of total ^{14}C and ^{15}N predictions, but noticeably improved the predictive quality and stability of MB-^{14}C and -^{15}N. Therefore, among the tested versions, the present paper proposes MOMOS-5 as the most accurate and the most consistent to describe labeling experiments during the first years of incubation. Modifications leading to MOMOS-6 were essentially carried out in order to model longer-term processes, including those associated with soil native organic matter (work in preparation). For that purpose, a stable humus compartment (HS) was introduced, which results from the slow stabilization of a small fraction of HL (H in MOMOS-5). In the paramo soils, MOMOS-6 HS includes a high amount of sequestered soil native C and

N. This labeling incubation allowed quantification of the ^{14}C and ^{15}N that has been sequestrated over a period of 2 years. This comparative study allows recommendation of the MOMOS-6 concept as a basis for simulating added and native SOM turnover in soil.

[41] **Acknowledgments.** TROPANDES INCO-DC program of the European Union (ERBIC18CT98-0263) supported this work. We are grateful to T. Carballas, CSIC-IIAG, Santiago de Compostela Spain, coordinator of the program, to A. Olivo, ICAE Mérida Venezuela, for her help in the field experiment, and to B. Buatois, CEFE-CNRS, Montpellier France and N. Marquez of the ICAE for the analysis of ^{14}C and ^{15}N.

References

Anderson, J. P. E., and K. H. Domsch (1978), A physiological method for the quantitative measurement of microbial biomass in soils, *Soil Biol. Biochem.*, *10*, 215–221.

Anderson, T. H., and K. H. Domsch (1993), The metabolic quotient for $CO_2(q_{CO2})$ as a specific activity parameter to assess the effect of environmental conditions such as pH on the microbial biomass of forests soil, *Soil Biol. Biochem.*, *25*, 393–395.

Bottner, P., and F. Warembourg (1976), Method for simultaneous measurement of total and radioactive carbon in soils, soil extracts and plant materials, *Plant Soil*, *45*, 273–277.

Brookes, P. C., J. F. Kragt, D. S. Powlson, and D. S. Jenkinson (1985), Chloroform fumigation and the release of soil nitrogen: The effects of fumigation time and temperature, *Soil Biol. Biochem.*, *17*, 831–835.

Chertov, O. G., and A. S. Komarov (1997), SOMM: A model of soil organic matter dynamics, *Ecol. Modell.*, *94*, 177–189.

Chimner, R. A., D. J. Cooper, and W. J. Parton (2002), Modeling carbon accumulation in Rocky Mountain fens, *Wetlands*, *22*, 100–110.

Cobelli, C., A. Lepschy, and G. Romanin-Jacur (1979), Structural identifiability of linear compartmental models, in *Theoretical Systems Ecology*, pp. 239–258, Academic, San Diego, Calif.

Franko, U., B. Oelschlägel, and S. Schenk (1995), Simulation of temperature-, water- and nitrogen dynamics using the model CANDY, *Ecol. Modell.*, *81*, 213–222.

Hansen, S., H. E. Jensen, N. E. Nielsen, and H. Svendsen (1991), Simulation of nitrogen dynamics and biomass production in winter wheat using the Danish simulation model DAISY, *Fertil. Res.*, *27*, 245–259.

Hénin, S., G. Monnier, and L. Turc (1959), Un aspect de la dynamique des matières organiques du sol, *C. R. Acad. Sci.*, *248*, 138–141.

Henriksen, T. M., and T. A. Breland (1999), Nitrogen availability effects on carbon mineralization, fungal and bacterial growth, and enzyme activities during decomposition of wheat straw in soil, *Soil Biol. Biochem.*, *31*, 1121–1134.

Jenkinson, D. S. (1990), The turnover of organic carbon and nitrogen in soil, *Philos. Trans. R. Soc. London, Ser. B.*, *329*, 361–368.

Jenkinson, D. S., and D. S. Powlson (1976), The effects of biocidal treatments on metabolism in soil: V. A method for measuring soil biomass, *Soil Biol. Biochem.*, *8*, 209–213.

Jenkinson, D. S., and J. H. Rayner (1977), The turnover of soil organic matter in some of the Rothamsted classical experiments, *Soil Sci.*, *123*, 298–305.

Joergensen, R. G. (1996), The fumigation-extraction method to estimate soil microbial biomass: Calibration of the k(EC) value, *Soil Biol. Biochem.*, *28*, 25–31.

Joergensen, R. G., and T. Mueller (1996), The fumigation-extraction method to estimate soil microbial biomass: Calibration of the k(EN) value, *Soil Biol. Biochem.*, *28*, 33–37.

Kätterer, T., M. Reichstein, O. Andrén, and A. Lomander (1998), Temperature dependence of organic matter decomposition: A critical review using literature data analyzed with different models, *Biol. Fertil. Soils*, *27*, 258–262.

Knorr, W., and M. Heimann (2001), Uncertainties in global terrestrial biosphere modeling: 1. A comprehensive sensitivity analysis with a new photosynthesis and energy balance scheme, *Global Biogeochem. Cycles*, *15*(1), 207–225.

Li, C., S. Frolking, and R. C. Harriss (1994), Modeling carbon biogeochemistry in agricultural soils, *Global Biogeochem. Cycles*, *8*(3), 237–254.

Lundquist, E. J., L. E. Jackson, K. M. Scow, and C. Hsu (1999), Change in microbial biomass and community composition, and soil carbon and nitrogen pools after incorporation of rye into three California agricultural soils, *Soil Biol. Biochem.*, *31*, 221–238.

Molina, J. A. E., C. E. Clapp, M. J. Shaffer, F. W. Chichester, and W. E. Larson (1983), NCSOIL, a model of nitrogen and carbon transformations in soil: Description, calibration and behavior, *Soil Sci. Soc. Am. J.*, *47*, 85–91.

Moorhead, D. L., W. S. Currie, E. B. Rastetter, W. J. Parton, and M. E. Harmon (1999), Climate and litter quality controls on decomposition: An analysis of modeling approaches, *Global Biogeochem. Cycles*, *13*, 575–589.

Mueller, T., L. S. Jensen, N. E. Nielsen, and J. Magid (1998), Turnover of carbon and nitrogen in a sandy loam soil following incorporation of chopped maize plants, barley straw and blue grass in the field, *Soil Biol. Biochem.*, *30*, 561–571.

Ocio, J. A., P. C. Brookes, and D. S. Jenkinson (1991), Field incorporation of straw and its effects on soil microbial biomass and soil inorganic N, *Soil Biol. Biochem.*, *23*, 171–176.

Pansu, M., and L. Thuriès (2003), Kinetics of C and N mineralization, N immobilization and N volatilization of organic inputs in soil, *Soil Biol. Biochem.*, *35*, doi:10.1016/S0038-0717(02)00234-1.

Pansu, M., Z. Sallih, and P. Bottner (1998), Modelling of soil nitrogen forms after organic amendments under controlled conditions, *Soil Biol. Biochem.*, *30*, 19–29.

Pansu, M., L. Thuriès, M. C. Larré-Larrouy, and P. Bottner (2003), Predicting N transformations from organic inputs in soil in relation to incubation time and biochemical composition, *Soil Biol. Biochem.*, *35*, doi:10.1016/S0038-0717(02)00285-7.

Parton, W. J., D. S. Schimel, C. V. Cole, and D. S. Ojima (1987), Analysis of factors controlling soil organic matter levels in great plains grasslands, *Soil Sci. Soc. Am. J.*, *51*, 1173–1179.

Paul, K. I., P. J. Polglase, and G. P. Richards (2003), Sensitivity analysis of predicted change in soil carbon following afforestation, *Ecol. Modell.*, *164*, 137–152.

Penning de Vries, F. W. T., D. M. Jansen, H. F. M. ten Berge, and A. Bakema (1989), *Simulation of Ecophysiological Processes of Growth in Several Annual Crops*, 271 pp., Pudoc, Wageningen, Netherlands.

Saggar, S., A. Parshotam, G. P. Sparling, C. W. Feltham, and P. B. S. Hart (1996), ^{14}C-labelled ryegrass turnover and residence times in soils varying in clay content and mineralogy, *Soil Biol. Biochem.*, *28*, 1677–1686.

Sallih, Z., and M. Pansu (1993), Modelling of soil carbon forms after organic amendment under controlled conditions, *Soil Biol. Biochem.*, *25*, 1755–1762.

Smith, P., et al. (1997), A comparison of the performance of nine soil organic matter models using datasets from seven long-term experiments, *Geoderma*, *81*, 153–225.

Thornley, J. H. M. (1991), A transport-resistance model of forest growth and partitioning, *Ann. Bot.*, *68*, 211–226.

Thornley, J. H. M., and E. L. Verberne (1989), A model of nitrogen flows in grassland, *Plant Cell Environ.*, *12*, 863–886.

Thuriès, L., M. Pansu, C. Feller, P. Herrmann, and J. C. Rémy (2001), Kinetics of added organic matter decomposition in a Mediterranean sandy soil, *Soil Biol. Biochem.*, *33*, doi:10.1016/S0038-0717(02)00003-7.

Thuriès, L., M. Pansu, M. C. Larré-Larrouy, and C. Feller (2002), Biochemical composition and mineralization kinetics of organic inputs in a sandy soil, *Soil Biol. Biochem.*, *34*, doi:10.1016/S0038-0717(02)00178-X.

Trinsoutrot, I., S. Recous, B. Mary, and B. Nicolardota (2000), C and N fluxes of decomposing C-13 and N-15 Brassica napus L.: Effects of residue composition and N content, *Soil Biol. Biochem.*, *32*, 1717–1730.

van Soest, P. J., J. B. Robertson, and B. A. Lewis (1991), Symposium: Carbohydrate methodology, metabolism, and nutritional implications in dairy cattle, *J. Dairy Sci.*, *74*(10), 3583–3597.

Verberne, E. L., J. Hassink, P. De Willigen, J. J. R. Groot, and J. A. Van Veen (1990), Modelling organic matter dynamics in different soils, *Neth. J. Agric. Sci.*, *38*, 221–238.

P. Bottner, Centre d'Ecologie Fonctionnelle et Evolutive, Centre National de la Recherche Scientifique, 1919 Route de Mende, F-34293 Montpellier Cedex 05 France. (bottner.pierre@wanadoo.fr)

K. Metselaar, Crop and Weed Ecology, Wageningen University and Research Centre, P.O. Box 430, NL-6700 AK, Wageningen, Netherlands. (henriette.drenth@wur.nl)

M. Pansu, Institut de Recherche pour le Développement, BP 64501, F-34394 Montpellier Cedex 05 France. (pansu@mpl.ird.fr)

L. Sarmiento, Instituto de Ciencias Ambientales y Ecológicas, Facultad de Ciencias, Universidad de los Andes, Mérida 5101, Venezuela. (lsarmien@ula.ve)